

10429
NACA TN 4095



NATIONAL ADVISORY COMMITTEE FOR AERONAUTICS

TECHNICAL NOTE 4095

AN ANALYSIS OF THE EFFECT OF SEVERAL PARAMETERS ON THE
STABILITY OF AN AIR-LUBRICATED HYDROSTATIC
THRUST BEARING

By William H. Roudebush

Lewis Flight Propulsion Laboratory
Cleveland, Ohio



Washington
October 1957

AFMCC
TECHNICAL LIBRARY
AFL 2811



NATIONAL ADVISORY COMMITTEE FOR AERONAUTICS

TECHNICAL NOTE 4095

AN ANALYSIS OF THE EFFECT OF SEVERAL PARAMETERS ON THE STABILITY OF
AN AIR-LUBRICATED HYDROSTATIC THRUST BEARING

By William H. Roudebush

SUMMARY

Equations are written which govern the motion of a gas-lubricated hydrostatic thrust bearing. The nonlinear equations are solved on a high-speed digital computer for air as the gas. Systematic investigations are made of the parameters involved in order to estimate their effect on stability.

A nonstable case is taken as a standard for comparison, and stability is achieved by properly varying any of several geometric and environmental parameters. The bearing pad volume and rigidity appear as prime controlling factors of stability. Smaller pad volumes and softer bearings result in more stable operation.

Higher temperatures reduce the weight flow and reservoir pressure required for a fixed load and clearance and favor stable operation by making a softer bearing.

INTRODUCTION

The possibility of using a gas as a bearing lubricant has attracted attention for many decades. Application has been confined, however, to certain installations where low viscosity was considered to be so important that the associated difficulties were not determinative. Such installations occur chiefly in instruments such as strain-gage balances, gyroscopes, and torque-measuring devices.

In recent years the second important property of gaseous lubricants, excellent thermal stability, has caused a renewed interest in the subject. An increasing number of applications is being encountered where extreme temperatures make conventional bearing lubricants impracticable. For this reason it becomes desirable to understand better the gas bearing and one of its chief deterrents, instability.

The present investigation considers a simple nonrotating thrust bearing consisting of two round flat disks of finite diameter separated by a thin film of air. The air under pressure enters the bearing clearance space at the center, flows to the periphery, and exhausts to the atmosphere. The resulting pressure distribution supports the bearing load.

The nonlinear differential equations governing the motion of the bearing when disturbed were solved on a high-speed digital computing machine. The solutions provide some information about the effect of certain parameters on the stability of the bearing. In addition, these solutions provide a means for checking the validity of more simplified solutions (e.g., ref. 1).

ANALYSIS

The simplifications made in order to solve a physical problem are generally dictated by the specific information that the solution is required to provide. The present solutions are intended to provide some information concerning the effect of several parameters on bearing stability. Accordingly, an effort is made to select those simplifications that might least affect the stability results.

Bearing Configuration and Operation

The geometry and nomenclature of the type of bearing investigated are shown in figure 1. Pressurized air comes from the constant-pressure reservoir through an orifice into the bearing pad. From the pad the air flows through the clearance space to the periphery of the bearing and exhausts to the atmosphere.

If the bearing load is increased slightly, the upper disk in figure 1 will move downward and decrease the clearance. This tends to decrease the weight flow out of the bearing periphery and also, by continuity, the weight flow into the bearing pad. Then the pressure drop decreases across the orifice so that the pad pressure increases, which tends to balance the increased load. In general, the bearing overshoots the new equilibrium clearance and begins to oscillate. This oscillation may lead to bearing collapse or may be damped out. The equations governing the oscillation are presented in the following section.

Basic Equations

The flows from the reservoir to the pad and from the pad to the periphery are considered separately and then are related through a continuity equation. All symbols are defined in appendix A.

The weight flow w_1 entering the bearing pad is given by (appendix B)

$$\left. \begin{aligned} w_1 &= \frac{3600Agp_R}{\sqrt{\frac{r-1}{2r}} RT_R} f^{1/r} \left(1 - f^{\frac{r-1}{r}}\right)^{1/2}, & f \leq f_{ch} \\ w_1 &= \frac{3600Agp_R}{\sqrt{\frac{r-1}{2r}} RT_R} f^{1/r} \left(1 - f^{\frac{r-1}{r}}\right)^{1/2}, & f_{ch} \leq f \leq 1 \\ w_1 &= \frac{-3600Agp_R}{\sqrt{\frac{r-1}{2r}} RT_S} f^{\frac{r-1}{r}} \left(1 - f^{\frac{1-r}{r}}\right)^{1/2}, & 1 \leq f \end{aligned} \right\} \quad (1)$$

In normal bearing operation f will probably be between f_{ch} and 1.

As the bearing oscillates, however, the orifice may choke (low pad pressure) or the flow may reverse in direction (high pad pressure). Both of these situations were encountered in the present investigation.

The flow outward from the pad radius to the bearing radius is computed from a modified form of the Navier-Stokes equation. The flow is assumed to be purely radial, the pressure is assumed to be a function of radius only, and the inertial forces are considered negligible in comparison with the viscous forces. With these assumptions, the following equations are obtained as developed in appendix B:

$$w_2 = \frac{3600\pi gh^3}{\mu RT_a \ln \frac{r_a}{r_s}} (p_s^2 - p_a^2) = \frac{3600\pi gh^3 p_R^2}{\mu RT_a \ln \frac{r_a}{r_s}} \left(f^2 - \frac{p_a^2}{p_R^2}\right) \quad (B12)$$

$$F_B = \frac{\pi(r_s^2 + r_a r_s + r_a^2)}{3} (p_s - p_a) = \frac{\pi(r_s^2 + r_a r_s + r_a^2) p_R}{3} \left(f - \frac{p_a}{p_R}\right) \quad (B16)$$

To preserve continuity, the difference between the weight flows into and out of the bearing is equated to the rate of increase of the weight in the bearing pad. Considering the change of state in the pad to occur adiabatically gives the result (appendix B)

$$w_1 - w_2 = 3600\pi r_s^2 \rho_{s,1} \left(\frac{f}{f_i}\right)^{1/r} \left(\frac{h+d}{rf} \frac{df}{dt} + \frac{dh}{dt}\right) \quad (2)$$

where the subscript i denotes conditions at initial equilibrium (time $t = 0$).

Now equation (2) with the substitution of equations (1) and (B12) gives one differential equation in f and h . A second differential equation is obtained by relating the forces acting on the bearing to the weight and acceleration of the bearing:

$$\frac{W}{12g} \frac{d^2 h}{dt^2} = F_B - F - \alpha \frac{dh}{dt} \quad (3)$$

or, by using equation (B16),

$$\frac{W}{12g} \frac{d^2 h}{dt^2} = \frac{\pi(r_s^2 + r_a r_s + r_a^2) P_R}{3} \left(f - \frac{p_a}{P_R} \right) - F - \alpha \frac{dh}{dt} \quad (4)$$

where F is the bearing loading function and $\alpha(dh/dt)$ is a drag term. The value of α is taken to be zero in the present analysis.

Equations (2) and (4) provide a system of two nonlinear differential equations in h and f . These equations were solved for various conditions on a high-speed digital computer.

General Considerations

In the present analysis the bearing is assumed to be in a state of initial equilibrium (denoted by subscript i) under a constant load F_i (fig. 2(a)). At time $t = 0$, a change in the loading function occurs (usually a step change to a value F_f) which puts the bearing temporarily out of equilibrium. The bearing then begins to hunt for the new equilibrium clearance h_f corresponding to the new load F_f . If the bearing settles out (fig. 2(b)) or oscillates with constant amplitude, it is said to be stable. If it oscillates with increasing amplitude, it is unstable. It is convenient to plot the behavior of the bearing as a dimensionless clearance parameter $(h - h_f)/(h_i - h_f)$ as shown in figure 2(c).

As a standard example, an unstable bearing configuration is selected. The pertinent bearing parameters are then varied one at a time in order to examine the ability of each to stabilize the bearing. The standard example has the following characteristics:

r_a , in.	6
r_s , in.	4
A , sq in.	0.003
d , in.	0.008
γ	1.4
W , lb	32.172
p_a , lb/sq in.	14.7
T , $^{\circ}R$	530
F_i , lb	500
h_i , in.	0.002
F_f , lb	550

With the characteristics selected, a solution proceeds as follows. First, certain preliminary computations are made:

(1) The initial pad pressure $p_{s,i}$ is found from equation (B16) by using the prescribed values of F_i , p_a , r_s , and r_a .

(2) The initial weight flow $w_{2,i}$ is found from equation (B12) by using the prescribed value of h_i and the computed value of $p_{s,i}$.

(3) Since $w_{1,i} = w_{2,i}$ (the system is in equilibrium), the required reservoir pressure p_R can be found from equation (1).

(4) The pressure ratio f_i is then obtained from $p_{s,i}$ and p_R .

(5) Although final equilibrium conditions may never be achieved, the values of $p_{s,f}$, h_f , and w_f , which would be obtained under a constant disturbance load F_f , are computed as above, except that p_R instead of h is now fixed. Second, with initial values of h_i and f_i now known, differential equations (2) and (4) are solved numerically to yield the bearing motion shown in figure 3.

In subsequent solutions the same process is carried out with F_i and h_i the same as in the standard example and with one of the bearing parameters changed. In this manner, systematic changes in important parameters can be made in an effort to improve the stability characteristics over those of the standard example. It is important to notice that no viscous damping force is included in the equations although such a force will be present in any real system. For this reason, the present analysis represents an extreme situation.

RESULTS

The results are presented mostly as plots of the bearing clearance parameter $(h - h_f)/(h_1 - h_f)$ against time as important bearing parameters are varied. Each plot contains the curve for the standard solution as a basis for comparison. The letters in parentheses on the plots are for use with table I which gives the results of preliminary calculations and the values of important parameters for each case.

Effect of Final Bearing Load F_f

The first parameter investigated was the disturbance load F_f . Final loads of 501, 550 (standard case), and 600 pounds were applied to a bearing having an initial load of 500 pounds in each case. The results are shown in figure 4.

Figure 4(a) shows the variation of the actual clearance h , while figure 4(b) shows the variation of the clearance parameter $(h - h_f)/(h_1 - h_f)$. Since h_f varied from one example to another, a clearance parameter such as this one is useful for comparison purposes. The curves of figure 4(b) are in close agreement over the first half cycle and deviate increasingly from there on. Since the agreement was sufficiently close, only one value of F_f (550 lb) is used throughout the remainder of the analysis.

Effect of Bearing Parameters

Pad depth. - It is generally believed (ref. 2) that reducing pad volume reduces the tendency to instability. A convenient way to do this is to make the pad depth smaller. In the standard case the pad depth is 0.008 inch, and the bearing is seriously unstable. Values of d of 0.004 and 0.002 inch are shown in figure 5 along with the standard case. The effect on clearance parameter variation is marked. Stability is actually achieved at $d = 0.002$ inch.

For sufficiently large values of d , the influence of pad depth is felt only during a displacement of the bearing, and its value does not affect the values of any other parameters at an equilibrium position (see table I). In this case, pad depth can be changed without altering the design operation of the bearing in any way.

Orifice area. - Increasing the area of the orifice joining the reservoir to the pad decreases the orifice resistance and reduces the reservoir pressure (table I) required to pass the initial weight flow.

(Remember that the initial load, pad radius, and clearance and, hence, the initial pad pressure and weight flow are fixed.) Thus, $f_1 = p_{s,1}/p_R$ is increased as orifice area increases. Also, it should be noted that $\Delta F/\Delta h$, a ratio comparable to a spring constant, decreases as the orifice area increases, which indicates a less rigid bearing (table I).

Figure 6 shows that the bearing is stabilized in this case by an increase in orifice area of less than 0.002 square inch. The bearing is quite stable at an area of 0.005 square inch.

Throughout the analysis, high values of f_1 and the corresponding softness of the bearing proved conducive to stability. On the other hand, high values of f_1 diminish the maximum equilibrium load that a bearing can carry with a fixed reservoir pressure. This may result in a design compromise between range and a degree of safeness with regard to stability.

Pad radius. - A decrease in the pad radius has a twofold effect on the bearing stability. The pad volume is decreased, and the initial pressure ratio f_1 is increased. Figure 7 indicates the variation of f_1 with pad radius for several values of orifice area. A number of factors contribute to the effect on f_1 . As pad radius decreases, the value of pad pressure necessary to support the fixed initial load increases slightly as shown in figure 8(a). This variation is determined completely by the variation of r_s (see eq. (B16)) and is independent of orifice area. From equation (B12) the weight flow varies with r_s explicitly and implicitly through p_s . Figure 8(b) shows this variation of weight flow. The rapid increase at large pad radii results in a rapid increase in reservoir pressure and, hence, the rapid decrease in f_1 indicated in figure 7. At the smaller orifice areas the effect of the weight flow change on the reservoir pressure is more marked.

Figure 9 shows the effect of decreasing pad radius on stability. As would be expected, the effect is favorable, and stable conditions are achieved with a pad radius of 3 inches. At a pad radius of 2 inches the oscillation is damped very quickly.

Temperature. - It has been shown that a higher temperature increases the load capacity of a bearing at a given weight flow (ref. 3). Or, as in the present case, the weight flow required to support a given load is reduced (eq. (B12)). The reservoir pressure is consequently reduced, and the value of f_1 is increased. As shown in table I, $\Delta F/\Delta h$ is decreased, which indicates a softer bearing. Figure 10 shows a favorable effect on stability. The general improvement resulting from increased temperature appears more significant in the case of higher loaded bearings, as is indicated in the section entitled "Higher loading."

Mass of system. - Figure 11 shows the effect of increasing the combined mass of bearing and load by a factor of 10. The starting frequency is decreased from about 285 to about 98 cycles per second. Thus, the frequency varies nearly inversely with the square root of the mass as in the case of a linear spring. The first half cycle dip is not as low for the larger mass, but the second half cycle peak is higher. The tendency toward instability is not appreciably affected in this example.

Other Effects

Linear applied load. - The step load used so far in the analysis represents an extreme condition never realized in practice. In order to gain an appreciation of the effect of this simplification, a number of linear load functions were used, each of which distributed the applied load over a longer time interval. The results, represented by the two cases shown in figure 12, indicate that there is no elimination of instability in this example. The bearing can be brought down quite close to its final equilibrium position if the load is applied very slowly. As soon as the load is fully on, however, and the forcing function is constant, the bearing begins to oscillate with increasing amplitude. It seems that the magnitude of the applied load and the way in which it is applied have little effect.

Isothermal compression. - Throughout the present analysis the air compression in the pad has been assumed to occur adiabatically. As this may not be true in the real case, a solution of the standard example was made in which the pad compression was assumed to occur isothermally, and the results are shown in figure 13. The isothermal case (appendix B) is the more unstable of the two.

Higher loading. - In many applications where an air bearing might prove useful, the bearing is subject to quite high loading. If the standard case is considered with the initial load and step load increased, the instability is heightened as shown in figure 14. The higher load raised the pad pressure. Since the initial clearance was the same, the weight flow was increased. Therefore, the orifice operated nearer to a choked condition (see table I), and $\Delta F/\Delta h$ was higher.

This may mean that the bearing must be designed for the maximum load that it will be expected to carry. Figure 15 shows the result of a very highly loaded (15,000 lb) bearing having the same outside diameter as the standard example with pad radius, depth, and orifice area chosen to eliminate instability. The small pad depth indicated in table I is achieved practically by making an annular pad instead of a circular one. The effective circular pad depth can be made a small fraction of the actual annular pad depth.

Very often high temperatures are present in the situations where the bearing loads are high. This is a help in reducing the weight flows required and in obtaining conditions conducive to stability. Figure 16 illustrates the favorable effect of increased temperature on a highly loaded bearing. The respective weight flows and reservoir pressures are indicated in table I. The higher temperature reduces the required weight flow to less than one-sixth and the reservoir pressure to less than one-third the original. The effect on stability is primarily due to the increase in f_1 and consequent softening of the bearing.

CONCLUDING REMARKS

In view of the simplifications made for the preceding analysis, experimental data are needed for substantiation of the results. Although such data are scarce at the present time, this situation may change in view of the potential that gas lubrication has for bearing applications of the future.

Certain conclusions can be drawn, however, from the analysis. Gas-lubricated bearings can evidently be designed to be stable, even under very high loads. Proper choice of pad volume and bearing rigidity is necessary. With the help of carefully obtained experimental data, either the derived equations or simpler linearized equations can probably be used to determine stable ranges of the important parameters. High temperatures are useful to the designer in lowering weight flow and reservoir pressure and raising the ratio of pad pressure to reservoir pressure.

Lewis Flight Propulsion Laboratory
National Advisory Committee for Aeronautics
Cleveland, Ohio, July 31, 1957

APPENDIX A

SYMBOLS

A	effective orifice area, sq in.
d	depth of pad, in.
F	force exerted on bearing by applied load, lb
F_B	force exerted on bearing by fluid, lb
ΔF	$F_i - F_f$, lb
f	ratio of pad pressure to reservoir pressure, p_s/p_R
f_{ch}	ratio of pad pressure to reservoir pressure when orifice is choked
g	acceleration due to gravity, ft/sec ²
h	bearing clearance, in.
Δh	$h_i - h_f$, in.
p	static pressure, lb/sq in. abs
R	gas constant, ft ² /(sec ²)(°R)
r	radius, in.
T	temperature, °R
t	time, sec
u	radial velocity, ft/sec
V_s	effective pad volume, $\pi r_s^2(h + d)$, cu in.
W	weight of combined bearing and load, lb
w	weight flow, lb/hr
w_1	weight flow into bearing pad, lb/hr
w_2	weight flow out of bearing pad, lb/hr
z	coordinate in direction of bearing axis, in.

α ratio of drag to velocity, lb-sec/ft

δ time interval, sec

γ ratio of specific heats

μ viscosity, lb-sec/sq ft

ρ density, lb/cu in.

Subscripts:

a condition at outer edge of bearing

f condition at final equilibrium, if reached

i condition at $t = 0$

R condition in reservoir

s condition at outer edge of pad

APPENDIX B

DEVELOPMENT OF EQUATIONS

The weight flow through an orifice from a reservoir of higher pressure p_H to one of lower pressure p_L is given by the equation (e.g., ref. 4)

$$w = 3600A \left\{ \frac{24\gamma g}{\gamma - 1} p_H^{\frac{\gamma+1}{\gamma}} \left(\frac{p_L}{p_H} \right)^{\frac{2}{\gamma}} \left[1 - \left(\frac{p_L}{p_H} \right)^{\frac{\gamma-1}{\gamma}} \right] \right\}^{1/2} \quad (B1)$$

Using the perfect gas law

$$p = \frac{12\rho RT}{g} \quad (B2)$$

in equation (B1) and simplifying give

$$w = \frac{3600Ag}{\sqrt{\frac{\gamma-1}{2\gamma} RT_H}} p_H \left(\frac{p_L}{p_H} \right)^{1/\gamma} \left[1 - \left(\frac{p_L}{p_H} \right)^{\frac{\gamma-1}{\gamma}} \right]^{1/2} \quad (B3)$$

where T_H is the temperature in the higher pressure reservoir. If $p_s \approx p_R$ in the case of the gas-lubricated bearing,

$$w_1 = \frac{-3600Ag}{\sqrt{\frac{\gamma-1}{2\gamma} RT_s}} p_s \left(\frac{p_R}{p_s} \right)^{1/\gamma} \left[1 - \left(\frac{p_R}{p_s} \right)^{\frac{\gamma-1}{\gamma}} \right]^{1/2} \quad (B4)$$

where the minus sign indicates that the flow is from the pad into the reservoir. With the notation $f = p_s/p_R$, equation (B4) can be written

$$w_1 = \frac{-3600Ag}{\sqrt{\frac{\gamma-1}{2\gamma} RT_s}} p_R f^{1-\frac{1}{\gamma}} \left(1 - f^{\frac{1-\gamma}{\gamma}} \right)^{1/2} \quad (B5)$$

If $p_s \leq p_R$, but the orifice is not choked, equation (B3) becomes

$$w_1 = \frac{3600Ag}{\sqrt{\frac{\gamma-1}{2\gamma} RT_R}} p_R f^{\frac{1}{\gamma}} \left(1 - f \frac{\gamma-1}{\gamma}\right)^{1/2} \quad (B6)$$

If the orifice is choked, the constant weight flow is given by

$$w_1 = \frac{3600Ag}{\sqrt{\frac{\gamma-1}{2\gamma} RT_R}} p_R f_{ch}^{\frac{1}{\gamma}} \left(1 - f_{ch} \frac{\gamma-1}{\gamma}\right)^{1/2} \quad (B7)$$

The weight flow out of the bearing periphery is obtained from the solution of a simplified Navier-Stokes equation. If the inertia terms are assumed to contribute little to the pressure gradient compared to the viscous force terms, the equation in cylindrical coordinates (fig. 1) is

$$\frac{\partial p}{\partial r} = \frac{\mu}{12} \frac{\partial^2 u}{\partial z^2} \quad (B8)$$

If p is assumed constant in the z -direction, equation (B8) can be integrated twice to give

$$u = \frac{6}{\mu} \frac{dp}{dr} z^2 + Bz + C$$

where the constants B and C are determined by the conditions that $u = 0$ for $z = 0$ and for $z = h$, so that

$$u = \frac{6}{\mu} \frac{dp}{dr} (z - h)z \quad (B9)$$

The weight flow w_2 is given by

$$w_2 = 3600(24\pi rp) \int_0^h u \, dz = \frac{-3600(24\pi rp)}{\mu} h^3 \frac{dp}{dr}$$

or

$$\frac{dp}{dr} = - \frac{\mu w_2}{3600(24\pi rp) h^3} \quad (B10)$$

By using equation (B2) and assuming isothermal flow, equation (B10) can be integrated from r_s to r , which gives

$$p^2 = \frac{-\mu w_2 R T_a}{3600 \pi g h^3} \ln \frac{r}{r_s} + p_s^2 \quad (B11)$$

With $p = p_a$ at $r = r_a$, w_2 is given by

$$w_2 = \frac{3600 \pi g h^3}{\mu R T_a \ln \frac{r_a}{r_s}} (p_s^2 - p_a^2) \quad (B12)$$

By using equation (B12), (B11) can be rewritten as

$$p^2 = p_s^2 - \left(\frac{p_s^2 - p_a^2}{\ln \frac{r_a}{r_s}} \right) \ln \frac{r}{r_s}$$

or

$$\frac{p}{p_s} = \left[1 - \frac{1 - \left(\frac{p_a}{p_s} \right)^2}{\ln \frac{r_a}{r_s}} \ln \frac{r}{r_s} \right]^{1/2} \quad (B13)$$

Figure 17 is a plot of p/p_s against r/r_s for several values of p_a/p_s and r_a/r_s . A reasonable approximation is obtained by taking p to vary with r as a straight line. With this simplification the expression for p becomes

$$p - p_a = \frac{p_s - p_a}{r_s - r_a} (r - r_a) \quad (B14)$$

The force F_B exerted on the upper plate of the bearing is given by

$$F_B = 2\pi \int_{r_s}^{r_a} (p - p_a) r \, dr + \pi r_s^2 (p_s - p_a) \quad (B15)$$

where the second term on the right is the contribution of the pad pressure which is considered to be uniform. Using equation (B14) in (B15) and integrating give

$$F_B = \frac{\pi}{3} (r_s^2 + r_a r_s + r_a^2) (p_s - p_a) \quad (B16)$$

The weight flow w_1 can be related to the weight flow w_2 through the law of mass conservation:

$$w_1 - w_2 = 3600 \frac{d(\rho_s V_s)}{dt}$$

or, with $V_s = \pi r_s^2 (h + d)$,

$$\frac{w_1 - w_2}{3600 \pi r_s^2} = (h + d) \frac{d\rho_s}{dt} + \rho_s \frac{dh}{dt} \quad (B17)$$

For reversible adiabatic compression,

$$\rho_s = \rho_{s,i} \left(\frac{p_s}{p_{s,i}} \right)^{\frac{1}{\gamma}}$$

and

$$\frac{d\rho_s}{dt} = \frac{1}{\gamma} \frac{\rho_{s,i}}{p_{s,i}^{1/\gamma}} p_s^{\frac{1-\gamma}{\gamma}} \frac{dp_s}{dt} \quad (B18)$$

Substituting equation (B18) into (B17) and simplifying give

$$\frac{w_1 - w_2}{3600 \pi r_s^2} = \rho_{s,i} \left(\frac{f}{f_i} \right)^{\frac{1}{\gamma}} \left(\frac{h + d}{r f} \frac{df}{dt} + \frac{dh}{dt} \right) \quad (B19)$$

The further assumption is made that the kinetic energy in the orifice flow is completely converted to internal energy in the bearing pad so that $T_{s,i} = T_R$. Substituting for w_1 and w_2 from equations (B6) and (B12) and further reducing give

$$\frac{dh}{dt} = \frac{-1}{f} \left\{ \frac{h + d}{r} \frac{df}{dt} - \left(\frac{f}{f_i} \right)^{\frac{\gamma-1}{\gamma}} \left[\frac{12A \sqrt{RT_R}}{\pi r_s^2 \sqrt{\frac{\gamma-1}{2\gamma}}} f^{\frac{1}{\gamma}} \left(1 - f^{\frac{\gamma-1}{\gamma}} \right)^{\frac{1}{2}} - \frac{12p_R \left(f^2 - \frac{p_a^2}{p_R^2} \right) h^3}{r_s^2 \ln \frac{r_a}{r_s}} \right] \right\} \quad (B20)$$

Similar reasoning for isothermal compression in the pad leads to

$$\frac{dh}{dt} = -\frac{1}{f} \left[(h + d) \frac{df}{dt} - \frac{12A\sqrt{RT_R}}{\pi r_s^2 \sqrt{\frac{\gamma-1}{2\gamma}}} f^{\frac{1}{\gamma}} \left(1 - f^{\frac{\gamma-1}{\gamma}} \right)^{\frac{1}{2}} + \frac{12p_R \left(f^2 - \frac{p_a}{p_R} \right) h^3}{r_s^2 \mu \ln \frac{r_a}{r_s}} \right] \quad (B21)$$

Either equation (B20) or (B21) is used as one of a pair of simultaneous differential equations in f and h . Another is obtained by equating the product of the mass and acceleration of the bearing to the forces acting upon it:

$$\frac{W}{12g} \frac{d^2h}{dt^2} = (F_B - F) - \alpha \frac{dh}{dt} \quad (B22)$$

where α is the ratio of drag to velocity. In the present analysis α is always taken to be zero. Substituting from equation (B16) gives the second equation in h and f :

$$\frac{d^2h}{dt^2} = \frac{4\pi g}{W} (r_s^2 + r_a r_s + r_a^2) p_R \left(f - \frac{p_a}{p_R} \right) - \frac{12g}{W} F \quad (B23)$$

Equations (B20) and (B23) are the principal equations of the present analysis.

REFERENCES

1. Richardson, H. H.: A Dynamic Analysis of Externally Pressurized Air Bearings. MS Thesis, M.I.T., 1955.
2. Mueller, Paul M.: Air Lubricated Bearings. Product Engineering - Annual Handbook of Product Design, McGraw-Hill Book Co., Inc., 1953, pp. J2-J5.
3. Pigott, J. D., and Macks, E. F.: Air Bearing Studies at Normal and Elevated Temperatures. Lubrication Eng., vol. 10, no. 1, Feb. 1954, pp. 29-33.
4. Liepmann, Hans Wolfgang, and Puckett, Allen E.: Introduction to Aerodynamics of a Compressible Fluid. John Wiley & Sons, Inc., 1947.

TABLE I. - BEARING PARAMETERS

Figure	F_i , lb	F_f , lb	h_i , in.	r_a , in.	d , in.	A , sq in.	r_s , in.	T , $^{\circ}$ R	W , lb	w_l , lb/hr	P_R , lb/sq in.	f_1	h_f , in.	$\Delta F/\Delta h$, lb/in.
5(a)	500	550	0.002	6	0.008	0.003	4	530	32.17	4.68	24.97	0.840	0.001882	4.24×10^5
5(b)	↓	↓	↓	↓	.004	↓	↓	↓	↓	↓	↓	↓	↓	↓
5(c)	↓	↓	↓	↓	.002	↓	↓	↓	↓	↓	↓	↓	↓	↓
6(a)	↓	↓	↓	↓	.008	↓	↓	↓	↓	↓	↓	↓	↓	↓
6(b)	↓	↓	↓	↓	↓	.004	↓	↓	↓	↓	23.21	.904	.001832	2.98
6(c)	↓	↓	↓	↓	↓	.005	↓	↓	↓	↓	22.40	.937	.001757	2.06
9(a)	↓	↓	↓	↓	↓	.003	4	↓	↓	↓	24.97	.840	.001882	4.24
9(b)	↓	↓	↓	↓	↓	↓	3	↓	↓	3.42	24.27	.918	.001787	2.35
9(c)	↓	↓	↓	↓	↓	↓	2	↓	↓	2.73	25.06	.953	.001505	1.01
10(a)	↓	↓	↓	↓	↓	↓	4	↓	↓	4.68	24.97	.840	.001882	4.24
10(b)	↓	↓	↓	↓	↓	↓	↓	630	↓	3.44	23.54	.892	.001847	3.27
10(c)	↓	↓	↓	↓	↓	↓	↓	730	↓	2.66	22.75	.922	.001800	2.50
11(a)	↓	↓	↓	↓	↓	↓	↓	530	↓	4.68	24.97	.840	.001882	4.24
11(b)	↓	↓	↓	↓	↓	↓	↓	↓	321.7	↓	↓	↓	↓	↓
14(a)	↓	↓	↓	↓	↓	↓	↓	↓	32.17	↓	↓	↓	↓	↓
14(b)	1,000	1,100	↓	↓	↓	↓	↓	↓	32.17	11.00	44.76	.609	.001911	11.23
15	15,000	16,500	↓	↓	.0013	.040	3	530	100	712.3	287.12	.843	.001703	50.5
16(a)	15,000	16,500	↓	↓	.0013	.010	3	530	100	645.66	976.00	.303	.001883	129.0
16(b)	15,000	16,500	↓	↓	.0013	.010	3	1660	100	103.17	289.47	.836	.001717	53.0

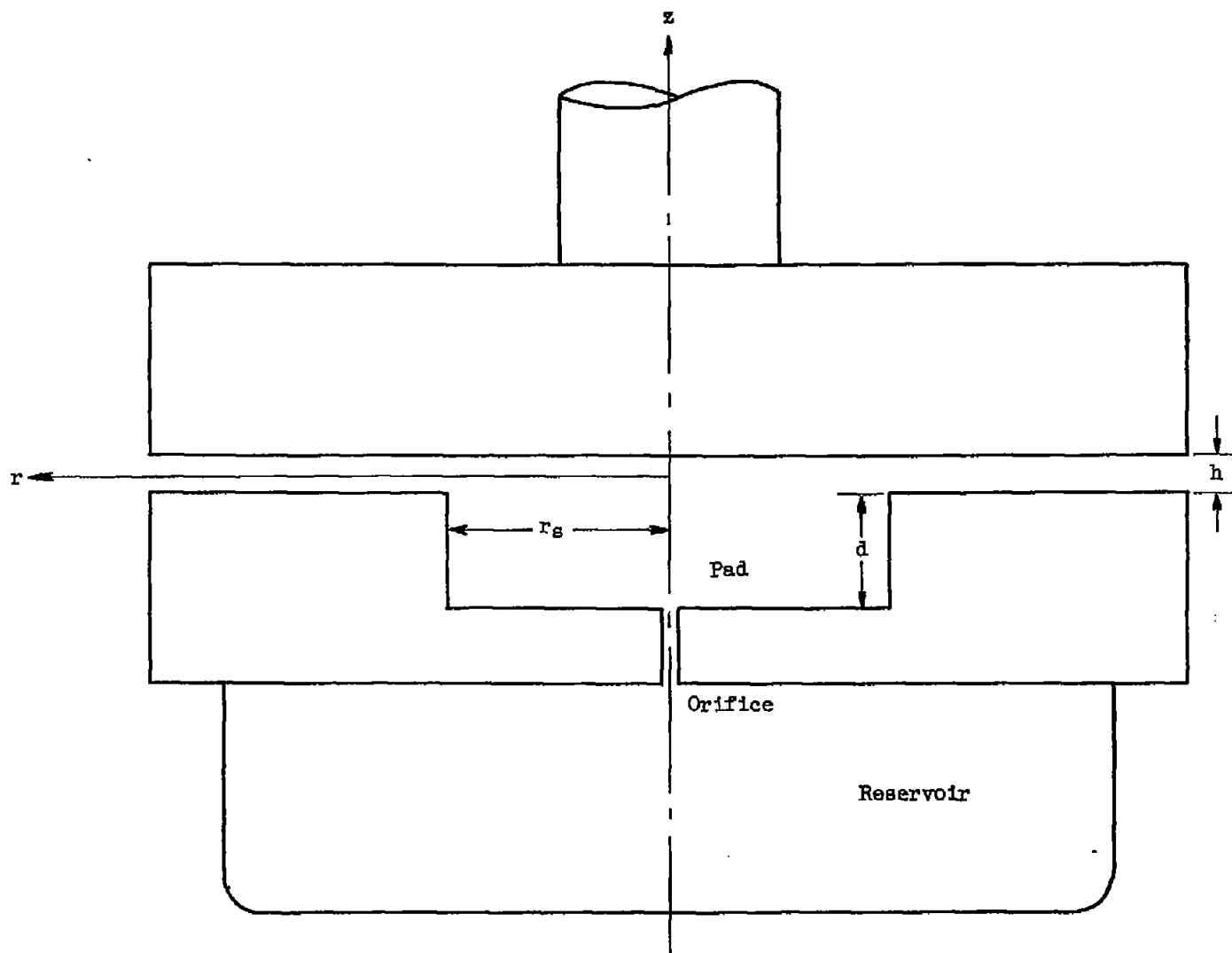
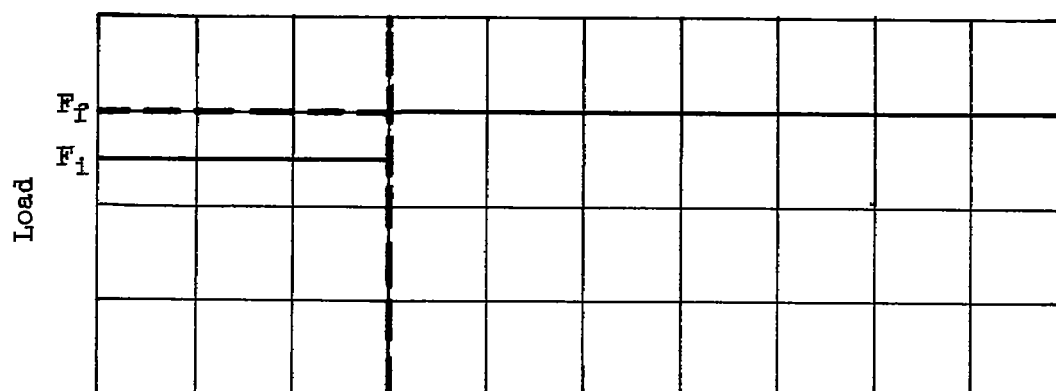
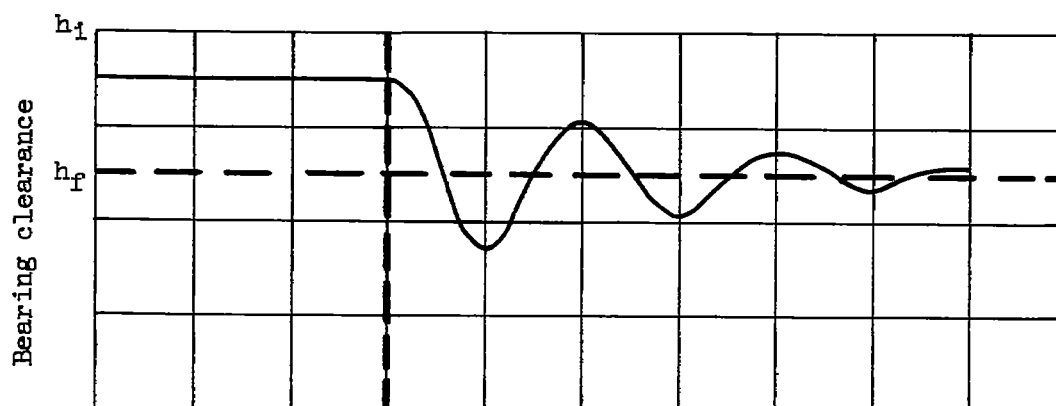


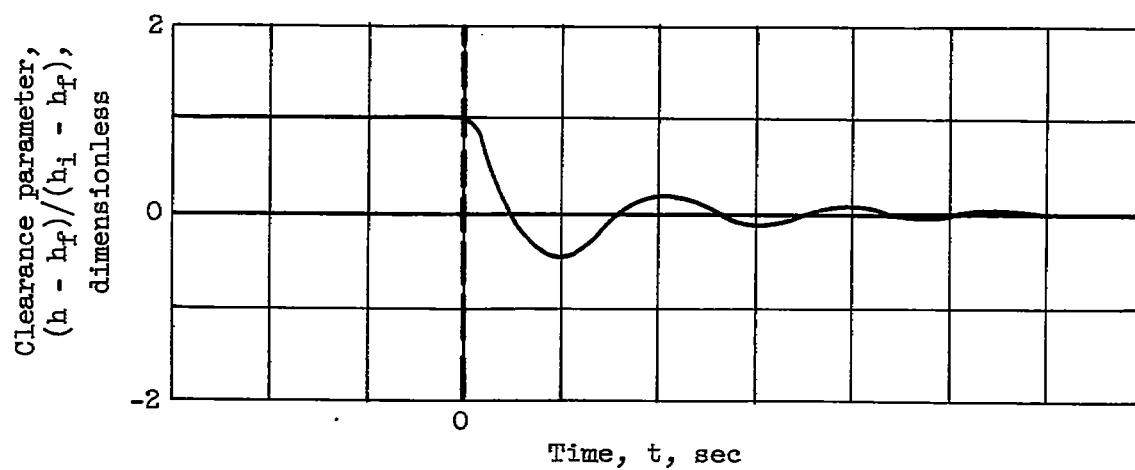
Figure 1. - Geometry of a simple circular pad thrust bearing.



(a) Load variation.



(b) Bearing clearance.



(c) Clearance parameter.

Figure 2. - Load variation and its effect on motion of bearing.

4579

CD-3 back

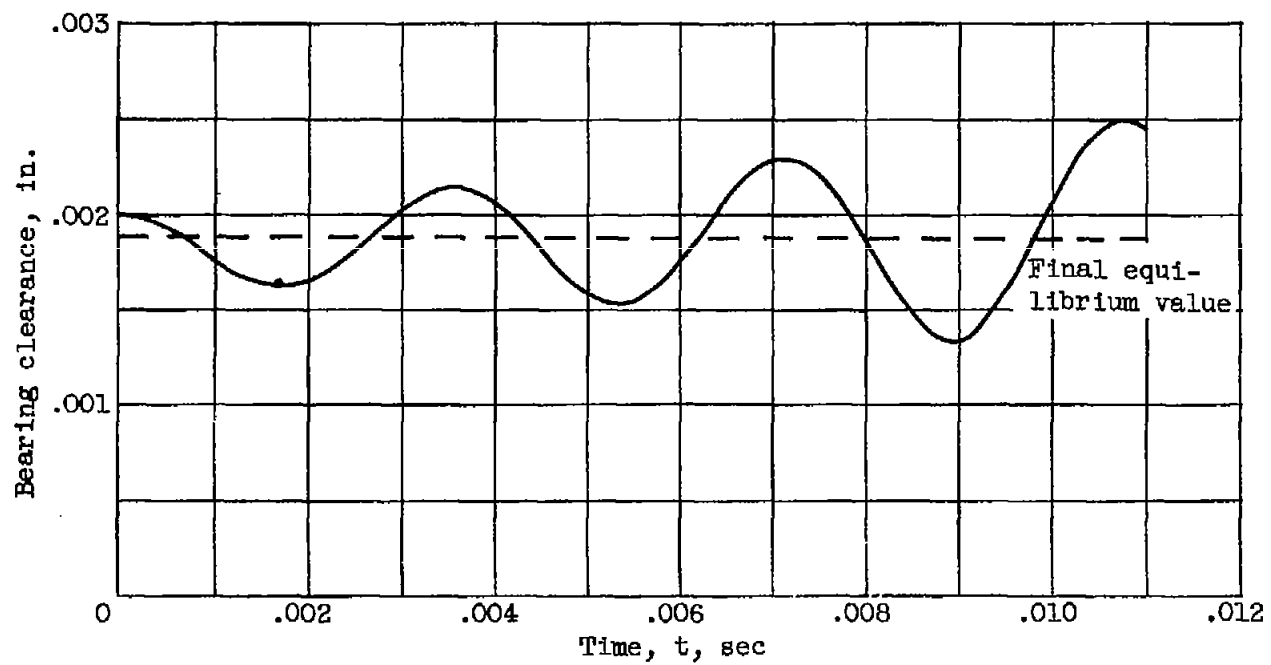
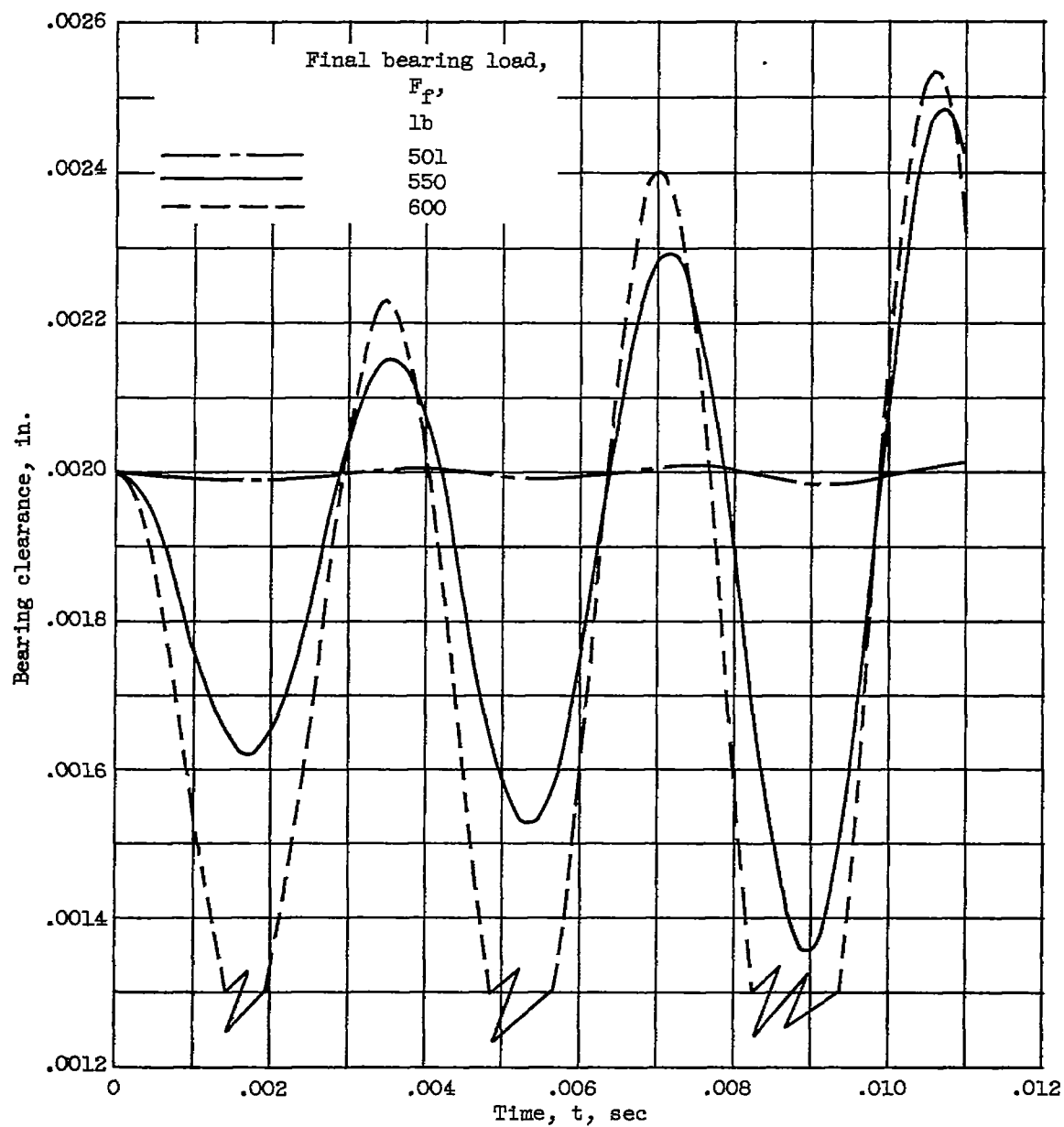
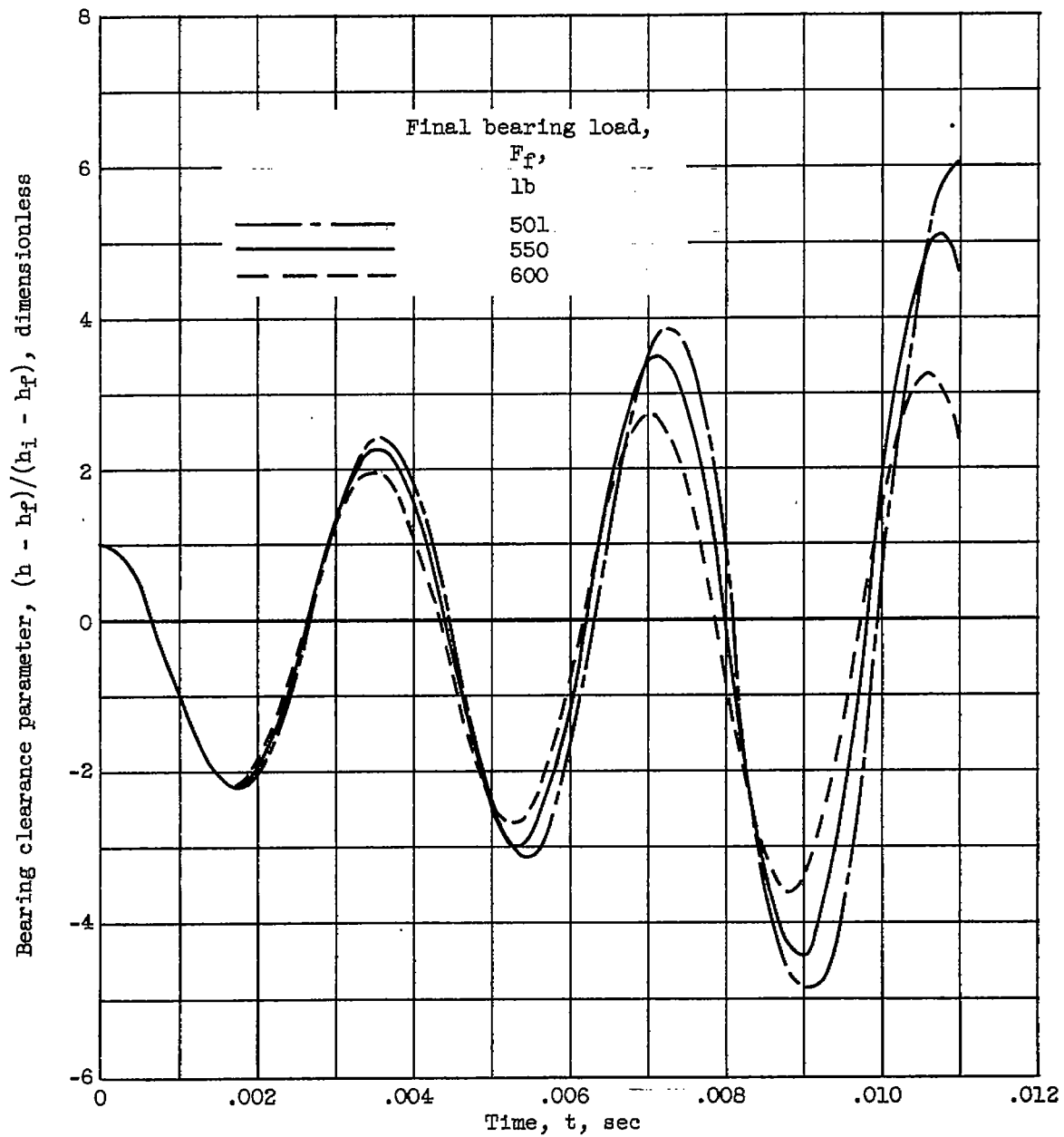


Figure 3. - Clearance variation for basic unstable bearing configuration.



(a) Bearing clearance.

Figure 4. - Effect of several values of final bearing load on time variation of bearing clearance and clearance parameter.



(b) Clearance parameter.

Figure 4. - Concluded. Effect of several values of final bearing load on time variation of bearing clearance and clearance parameter.

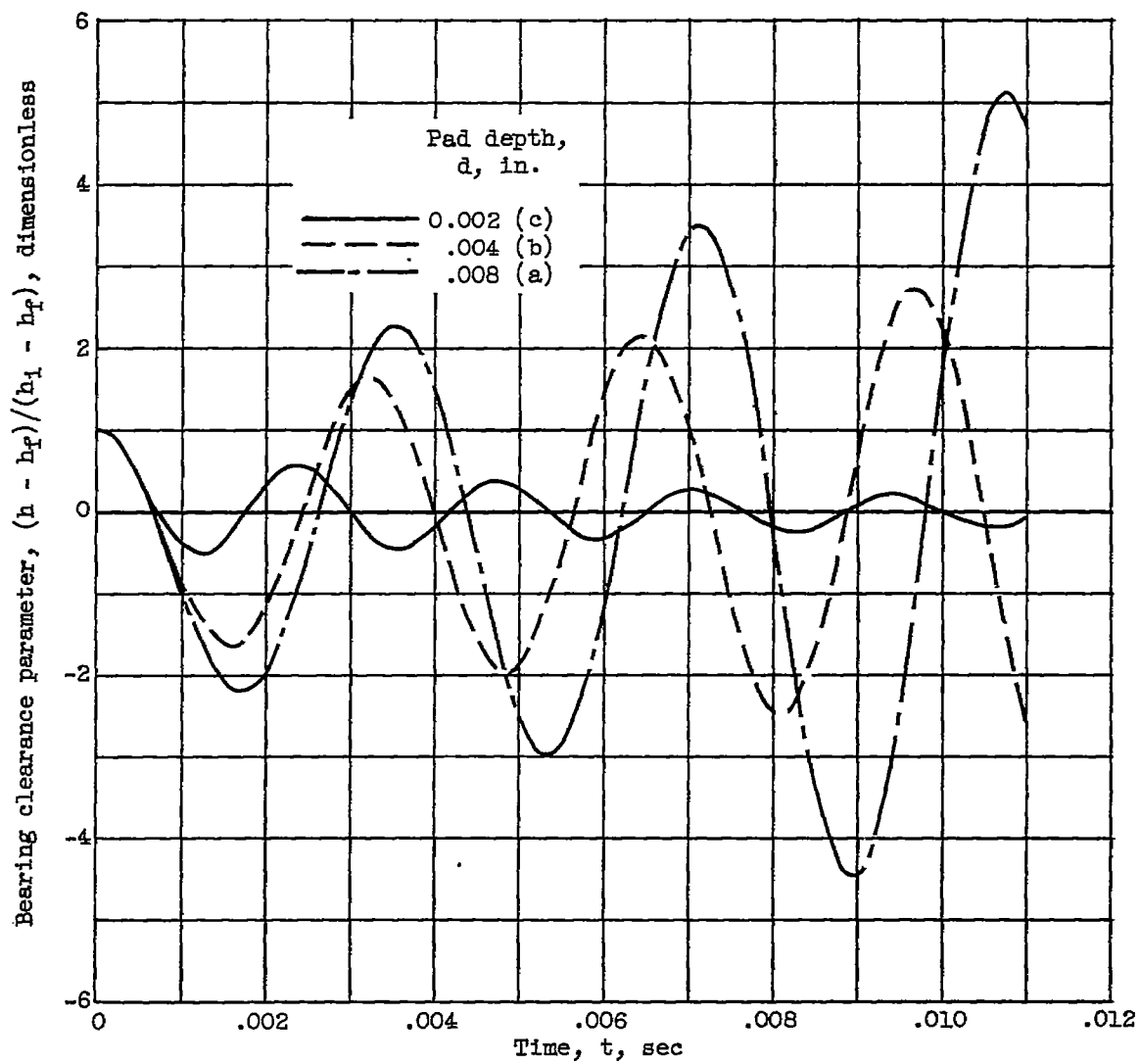


Figure 5. - Effect of variation of pad depth on clearance parameter.

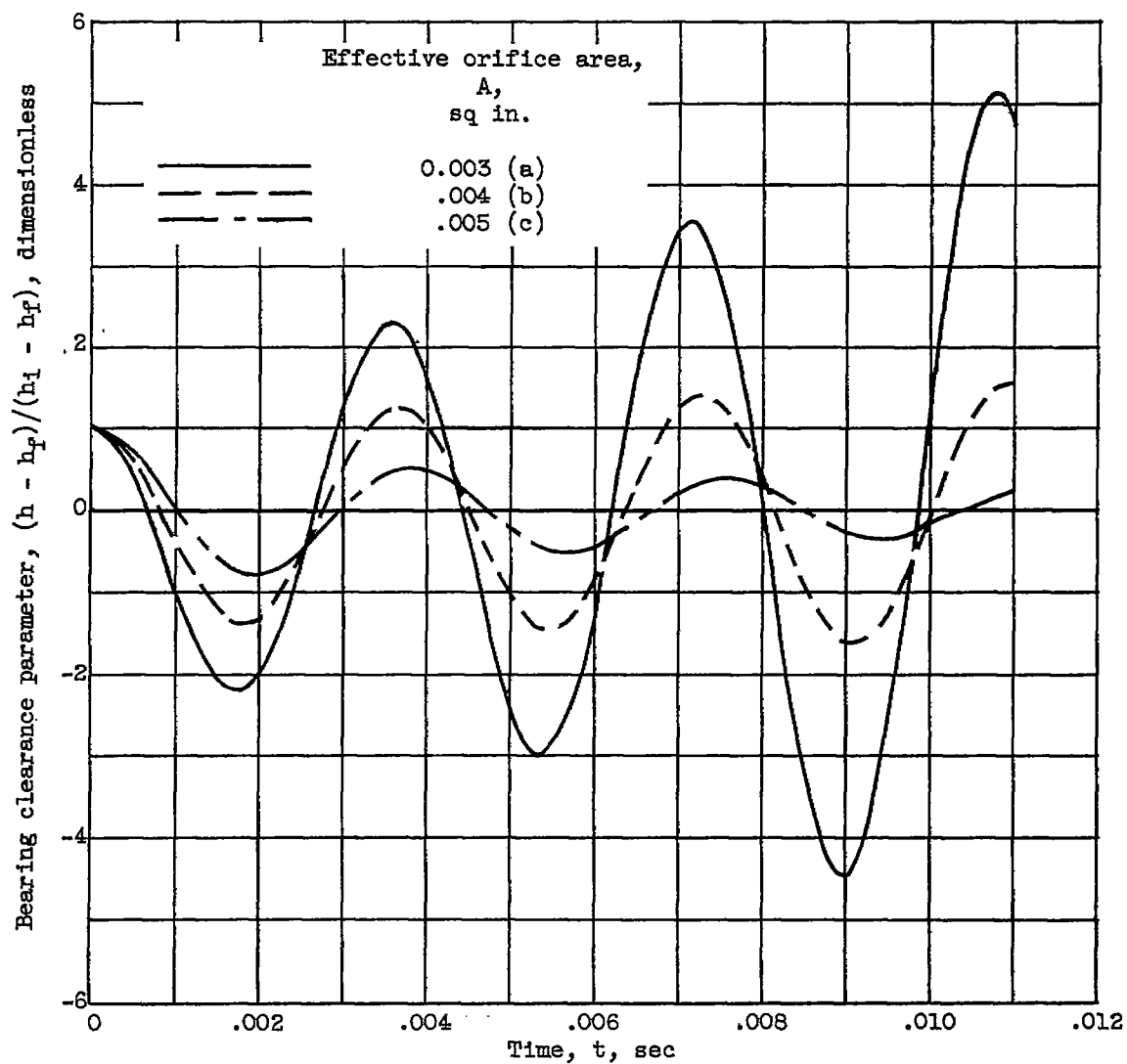


Figure 6. - Effect of variation of orifice area on clearance parameter.

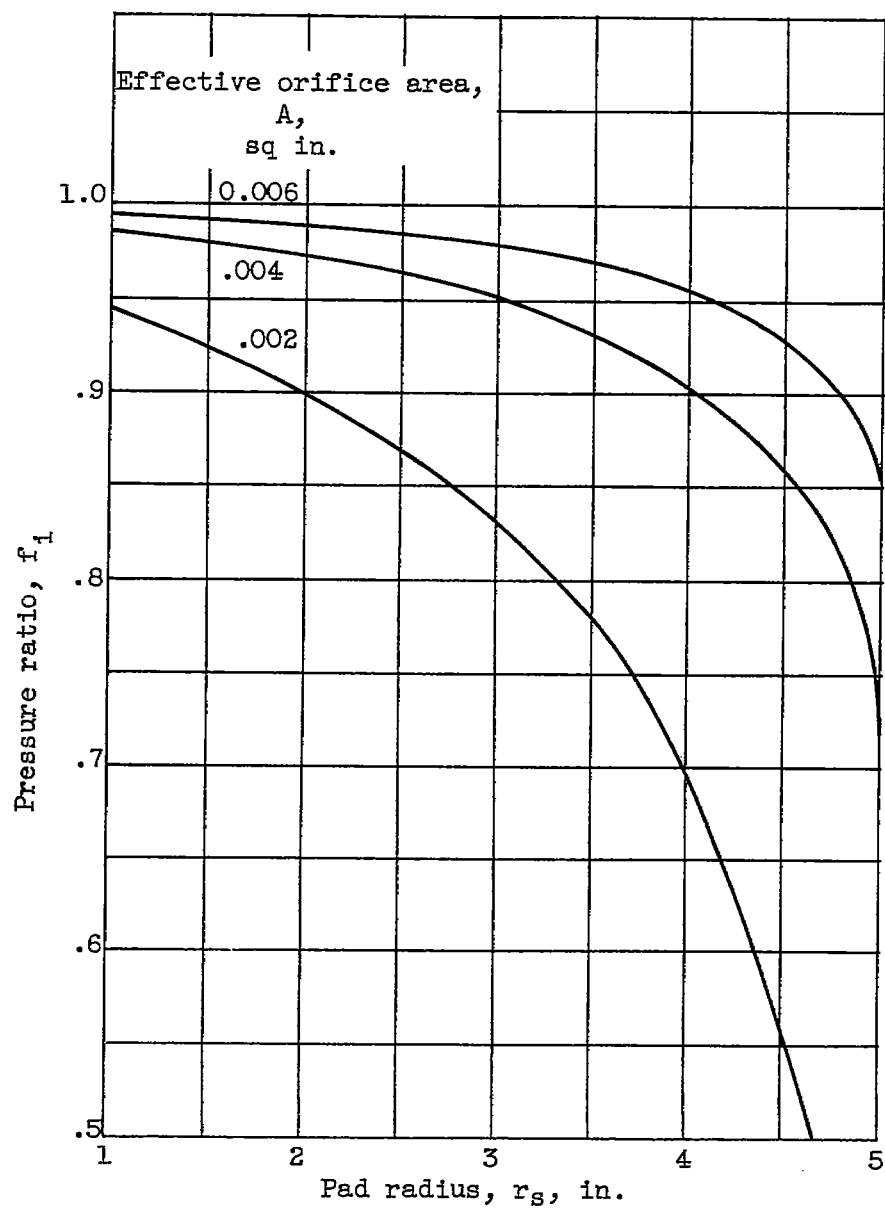
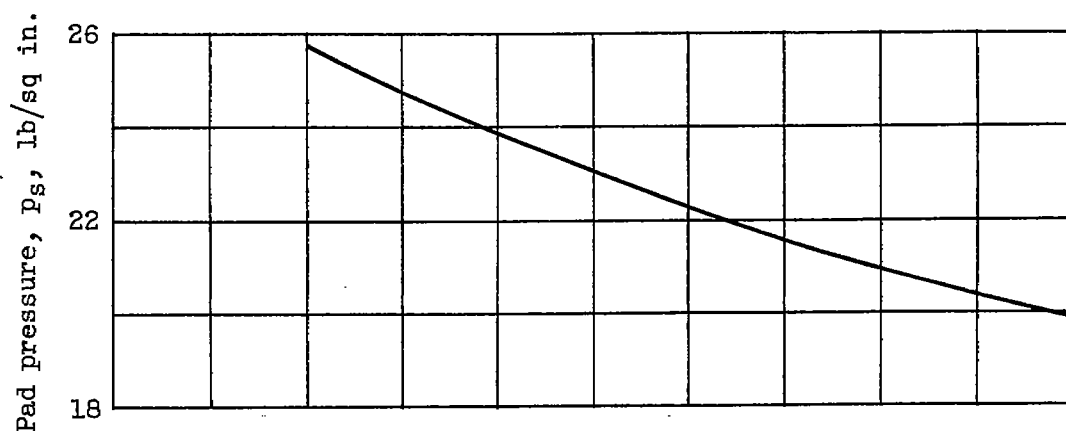
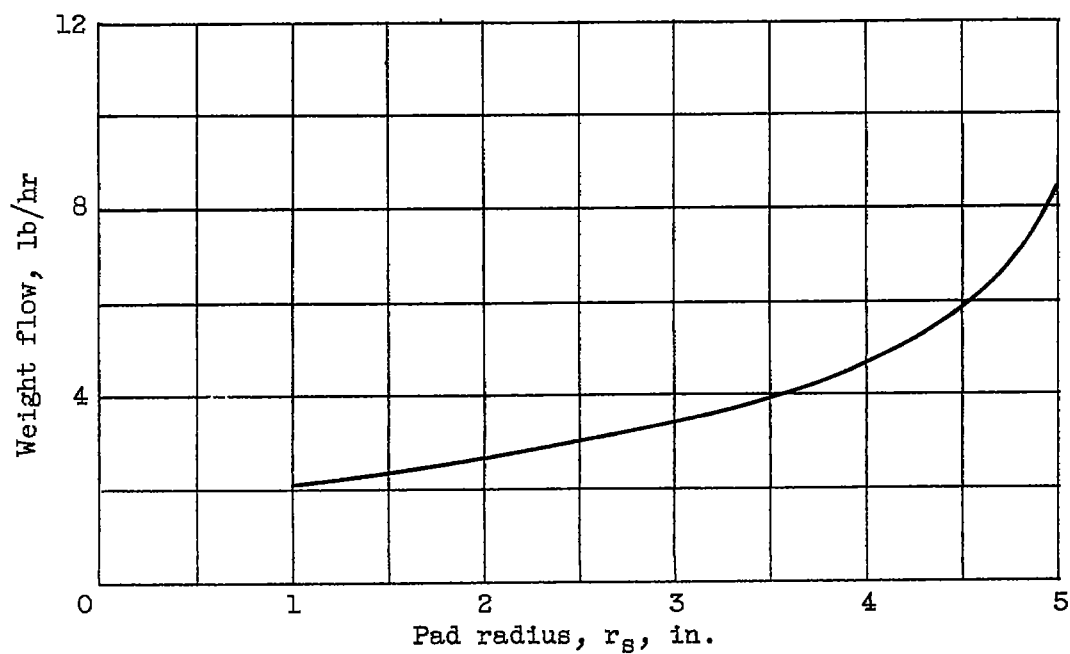


Figure 7. - Effect of pad radius on ratio of pad pressure to reservoir pressure. $F_1 = 500$ pounds; $h_1 = 0.002$ inch; $r_a = 6$ inches.



(a) Pad pressure.



(b) Weight flow.

Figure 8. - Effect of pad radius on pad pressure and weight flow. $F_1 = 500$ pounds; $h_1 = 0.002$ inch; $r_a = 6$ inches.

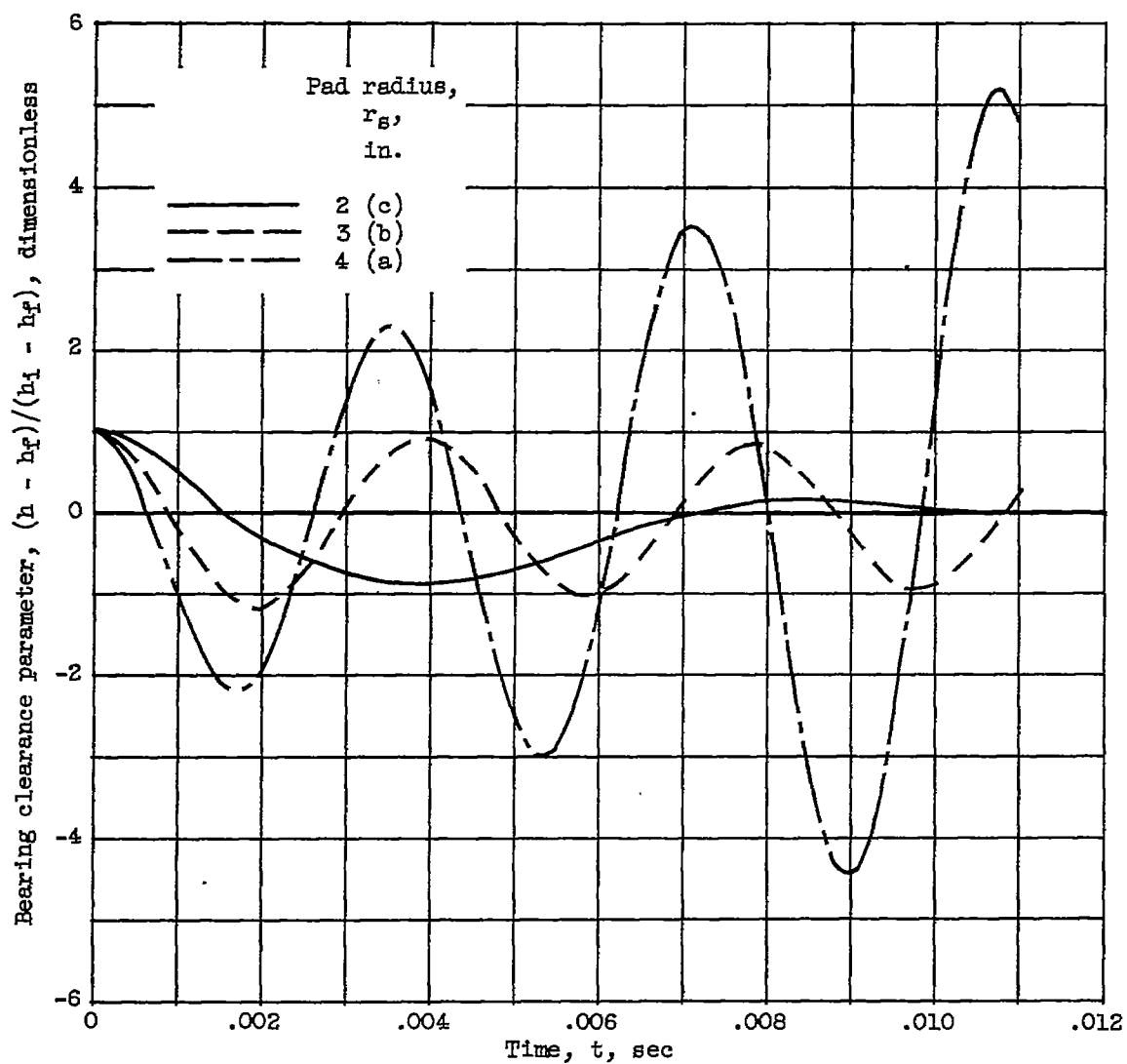


Figure 9. - Effect of variation of pad radius on clearance parameter.

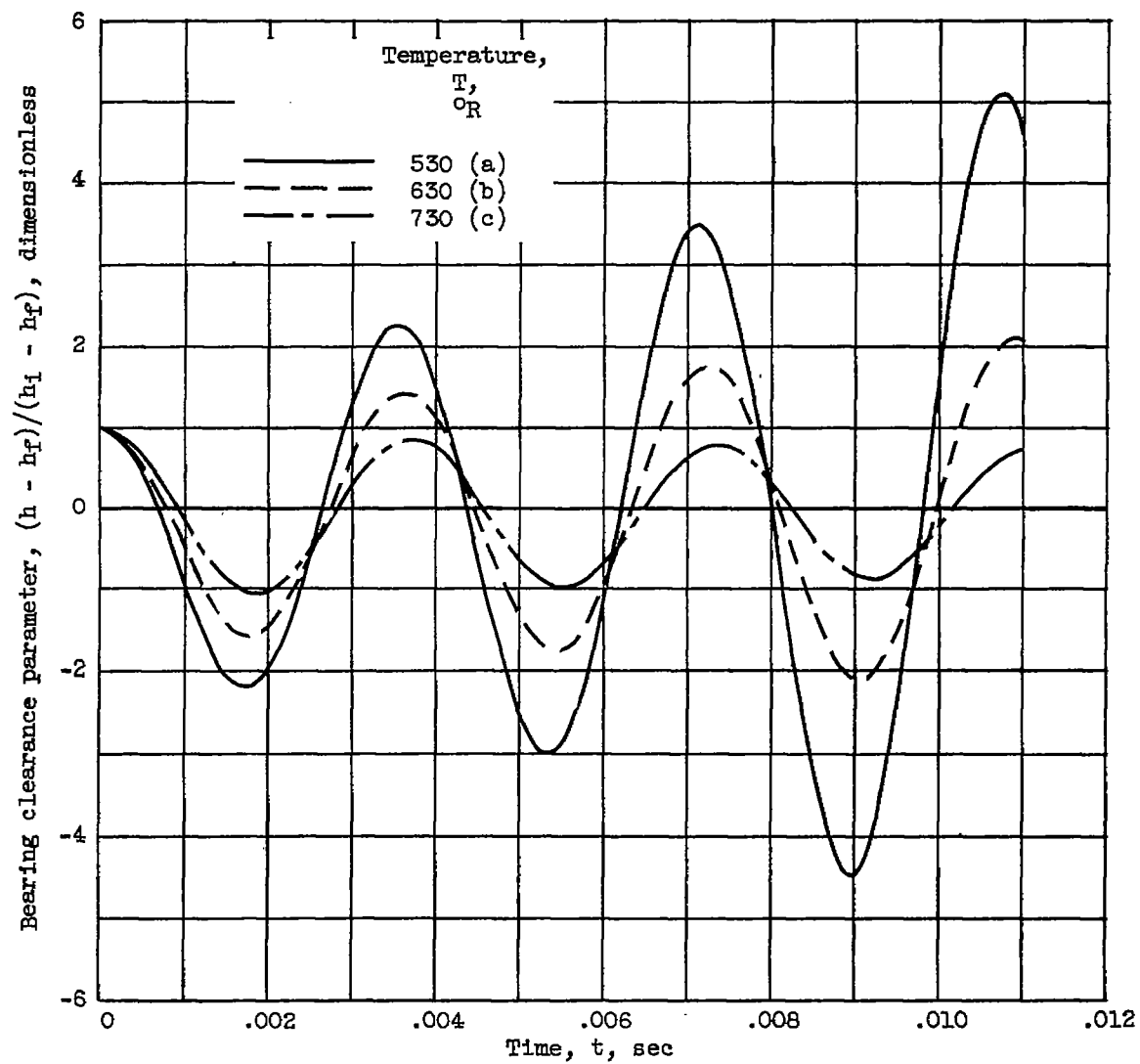


Figure 10. - Effect of variation of air temperature on clearance parameter.

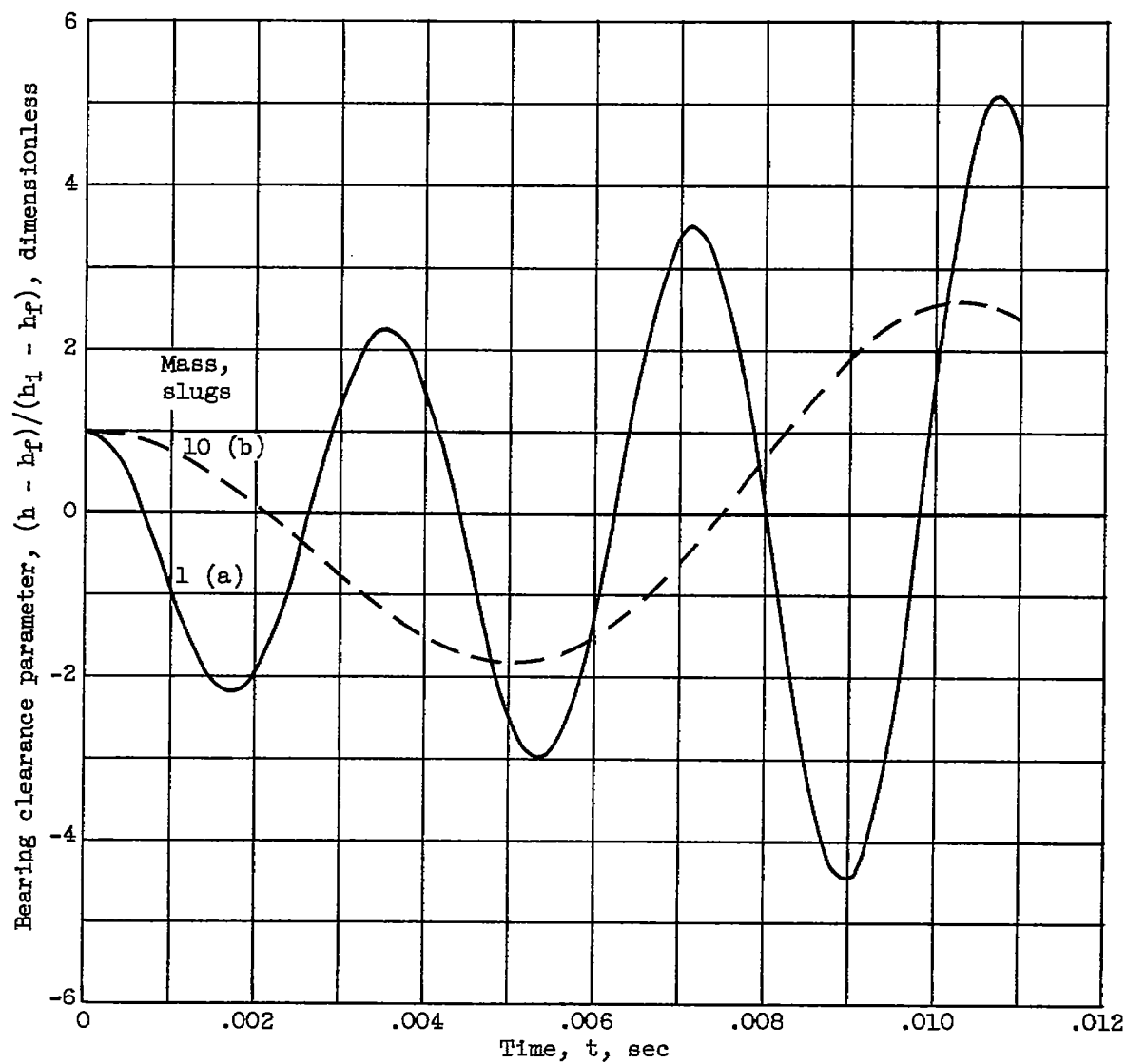


Figure 11. - Effect of variation of mass on clearance parameter.

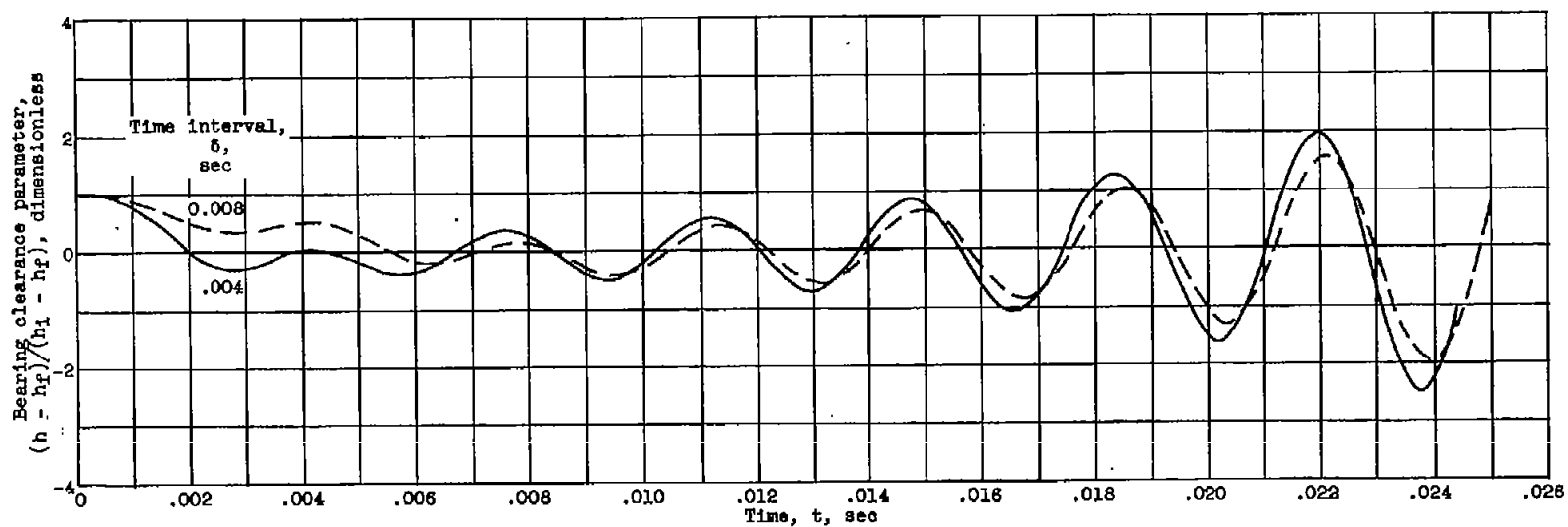


Figure 12. - Effect on clearance parameter variation due to linear load application over time interval. $F_1 = 500$ pounds; $h_1 = 0.002$ inch; $r_a = 6$ inches; $r_s = 4$ inches; $A = 0.003$ inch; $d = 0.008$ inch; $F_f = 550$ pounds.

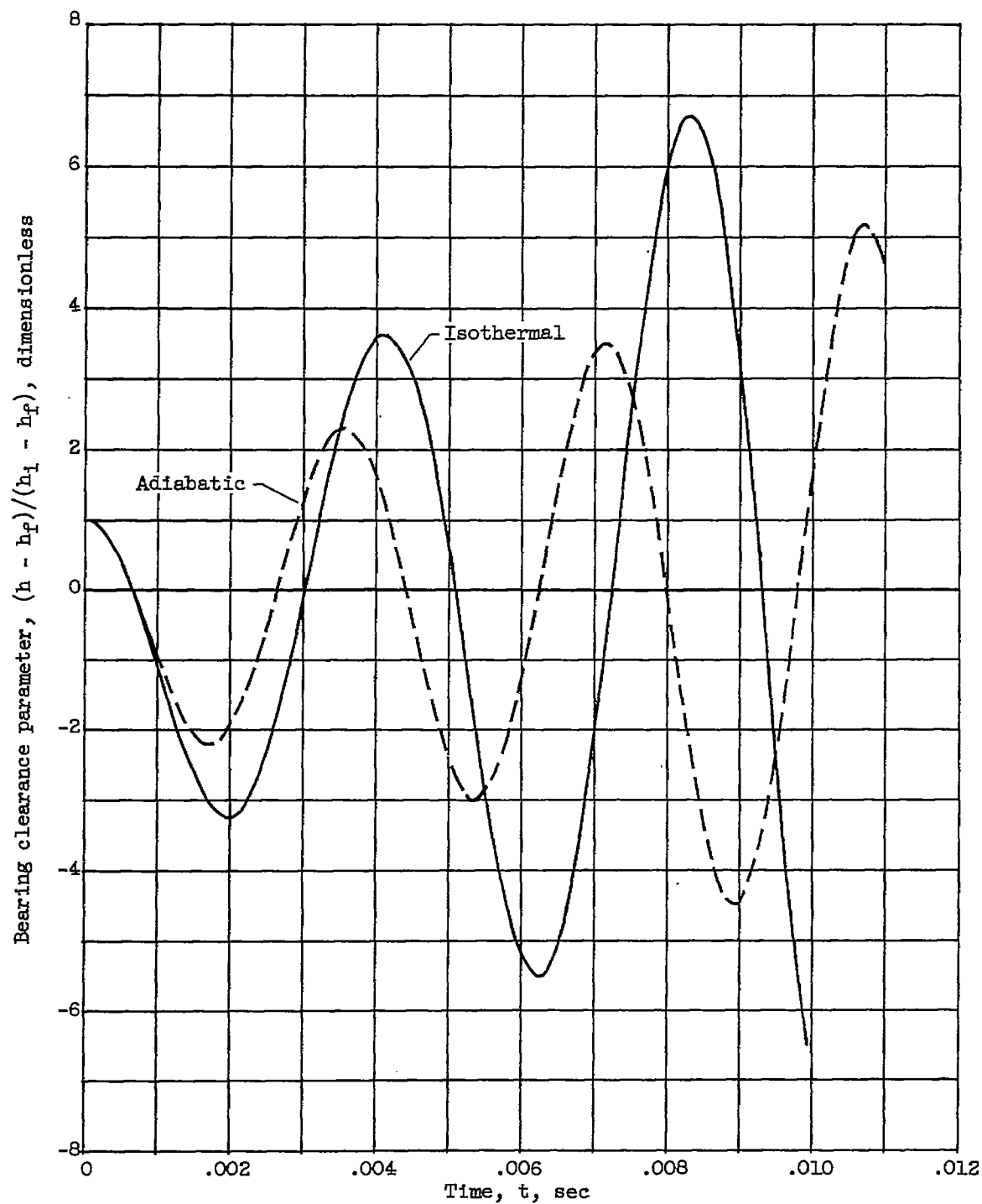


Figure 13. - Comparison of effects on clearance parameter of adiabatic and isothermal compression in bearing pad.

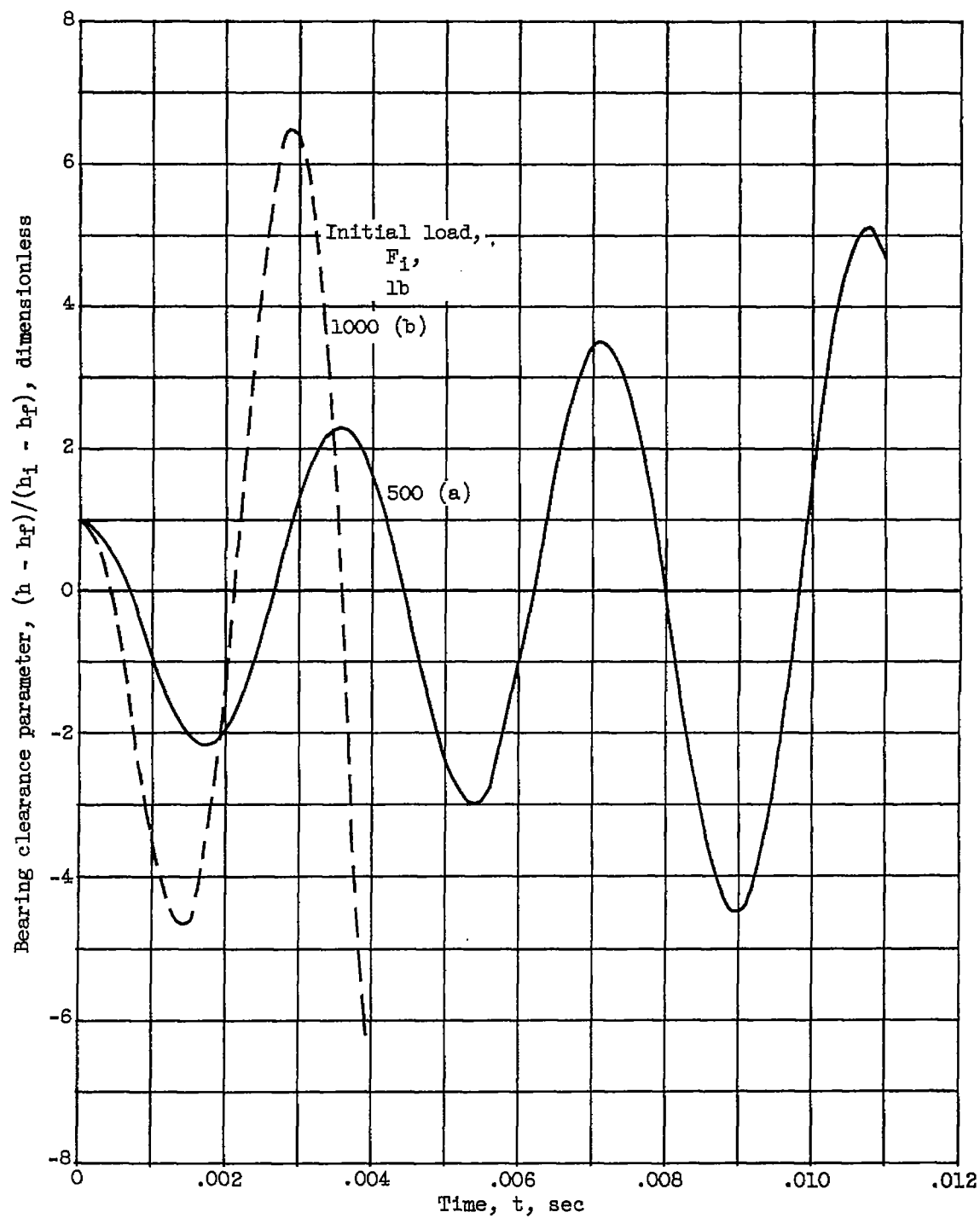


Figure 14. - Effect of variation of initial loading on clearance parameter.

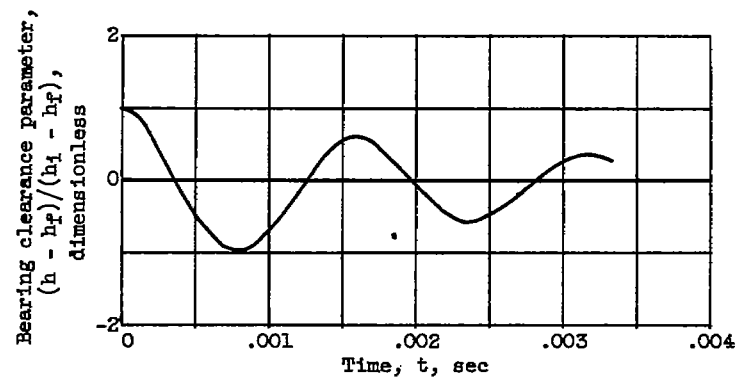


Figure 15. - Clearance parameter variation of a stable high-load bearing. $F_1 = 15,000$ pounds.

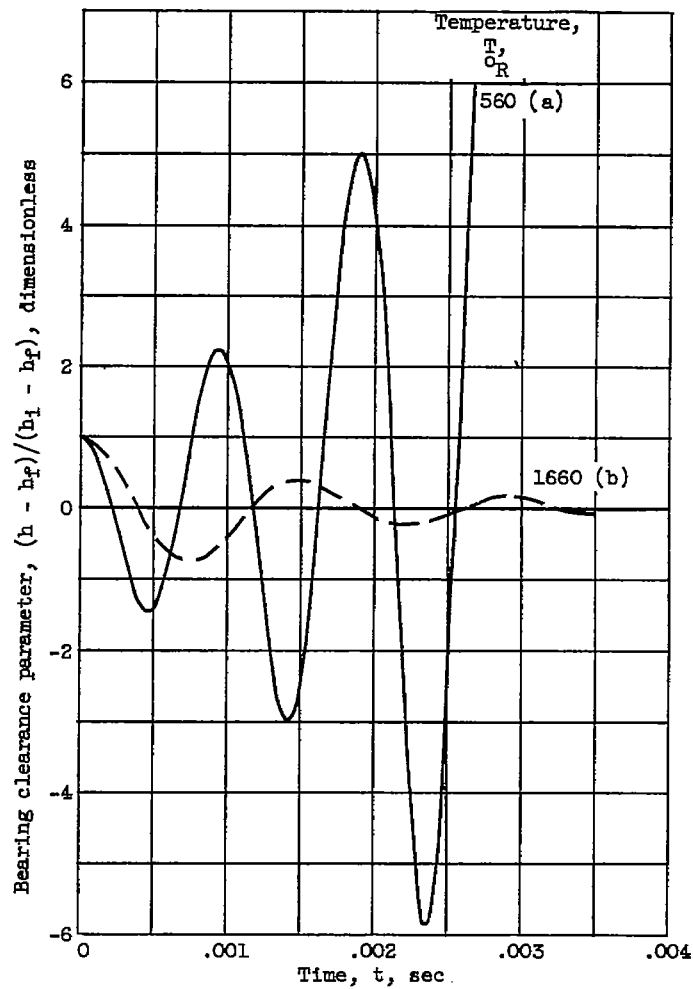
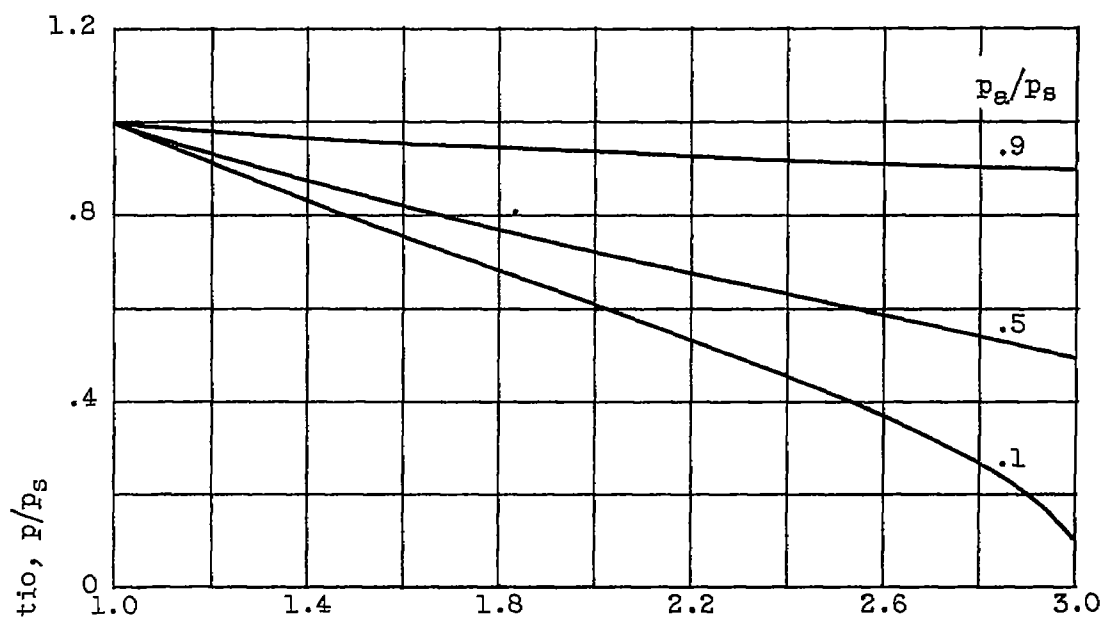
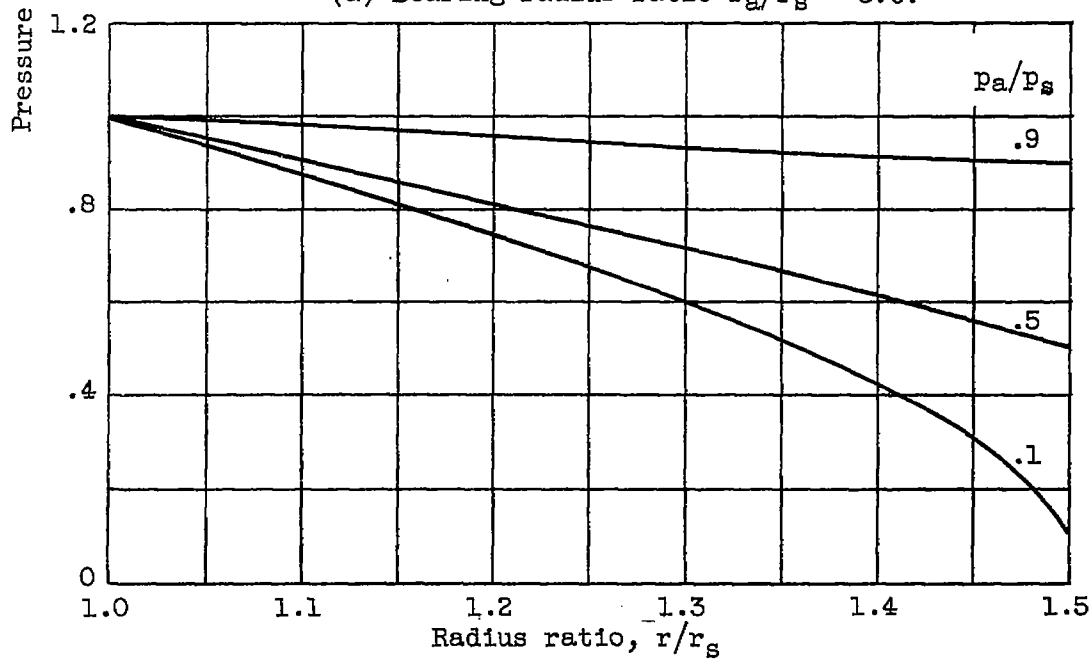


Figure 16. - Effect of temperature on clearance parameter variation for high-load bearing. $F_1 = 15,000$ pounds.



(a) Bearing radius ratio $r_a/r_s = 3.0$.



(b) Bearing radius ratio $r_a/r_s = 1.5$.

Figure 17. - Local pressure ratio as function of radius ratio for several conditions.